

# Semiconductor-Type MEMS Gas Sensor for Real-Time Environmental Monitoring Applications

Seung Eon Moon, Nak-Jin Choi, Hyung-Kun Lee, Jaewoo Lee, and Woo Seok Yang

**Low power consuming and highly responsive semiconductor-type microelectromechanical systems (MEMS) gas sensors are fabricated for real-time environmental monitoring applications. This subsystem is developed using a gas sensor module, a Bluetooth module, and a personal digital assistant (PDA) phone. The gas sensor module consists of a NO<sub>2</sub> or CO gas sensor and signal processing chips. The MEMS gas sensor is composed of a microheater, a sensing electrode, and sensing material. Metal oxide nanopowder is drop-coated onto a substrate using a microheater and integrated into the gas sensor module. The change in resistance of the metal oxide nanopowder from exposure to oxidizing or deoxidizing gases is utilized as the principle mechanism of this gas sensor operation. The variation detected in the gas sensor module is transferred to the PDA phone by way of the Bluetooth module.**

**Keywords:** Gas sensor, metal oxide, nanopowder, microheater.

## I. Introduction

Wireless sensor networks (WSNs) have many attractive applications, inevitably making them an important and growing market in the near future [1]. Inventory systems, logistics management, healthcare, domestic control, and environmental monitoring are only a few examples of WSN applications. Such sensor networks require the combination of a huge number of inexpensive small sensors with wireless communication and ultra-low power consumption. Communication can be direct with base stations or in multihop networks that are configured ad hoc.

Air quality control is the main aspect in the field of environmental monitoring, as respiratory organ diseases are mainly ascribed to poor air quality. Atmospheric environmental standards are somewhat different in each country, and air quality can be expressed through the concentration of several pollutants, such as carbon monoxide, sulphur dioxide, nitrogen dioxide, and ozone. The threshold values specified for these pollutants by the European Environment Agency (EEA) assure indoor air quality of 10 mg/m<sup>3</sup>, 350 µg/m<sup>3</sup>, 40 µg/m<sup>3</sup>, and 120 µg/m<sup>3</sup>, respectively [2]. Among these, the sensing of carbon monoxide and nitrogen dioxide in the atmosphere has been assumed to be of great importance owing to the serious problem of atmospheric air pollution caused by automobile exhaust and other sources.

Various types of gas sensors with different operational methods have been developed in recent years. In spite of their high operating temperature, resistive metal oxide sensors play a significant role because of their low cost and high sensitivity. Having a smaller size than electrochemical and optical gas sensors and lower power consumption than optical gas sensors are the other merits of WSN applications [3]-[12].

---

Manuscript received Nov. 26, 2012; revised June 3, 2013; accepted July 2, 2013.

This work was supported by the Technology Innovation Program (Innovation Cluster Program) through the Korea Innovation Cluster Foundation funded by the Ministry of Knowledge Economy (MKE, Korea) and by the IT R&D program of the MKE/KEIT [10035570, Development of self-powered smart sensor node platform for Smart & Green building].

Seung Eon Moon (phone: +82 42 860 5603, semoon@etri.re.kr), Nak-Jin Choi (choinj1@etri.re.kr), Hyung-Kun Lee (hklee@etri.re.kr), Jaewoo Lee (jwlee@etri.re.kr), and Woo Seok Yang (wsyang68@etri.re.kr) are with the Components & Materials Research Laboratory, ETRI, Daejeon, Rep. of Korea.

<http://dx.doi.org/10.4218/etrij.13.1912.0008>

Metal oxide nanopowders for gas sensors present higher sensitivities and shorter recovery times than conventional metal oxide film sensors, owing to the effects of their size reduction [13]-[17]. For these reasons, metal oxide nanopowders are believed to be very promising in the development of a new generation of metal oxide sensors with improved properties.

In this paper, we present the design and experiment results of a semiconductor-type microelectromechanical systems (MEMS) gas sensor utilizing a metal oxide nanopowder gas sensor for the detection of carbon monoxide and nitrogen dioxide for a wireless environmental monitoring subsystem, which is small enough to be directly attached to wireless nodes, such as a Bluetooth head set, and operate using a personal digital assistant (PDA). This system is composed of four major parts: a gas sensor, sensor-interrogating and digital-interfacing printed circuit boards (PCBs), a Bluetooth module, and a real-time data acquisition program executed on a PDA. The actual performances of our sensor chip and wireless environmental monitoring subsystem are evaluated for carbon monoxide and nitrogen dioxide gases. These results are described and discussed below, along with the embodiment processes of the PDA-based wireless environmental monitoring subsystem.

## II. Fabrication and Measurements

### 1. Metal Oxide MEMS Gas Sensor

For rapid gas sensing and desorption, a microheater is necessary for high-temperature operation. In a microheater structure, the two semicircular Pt heaters are connected to the power supply and are embedded in the membrane, which consists of  $\text{SiO}_2$  and  $\text{SiN}_x$  thin films. The resistance of each heater becomes electrically equal, and each heater line is divided in half by the heat-spreading circular line. The generated heat diffuses through the heat spreader to promote thermal uniformity in the center area, which is thermally isolated by air using a membrane structure. The power consumption of the microheater device is simulated using commercial finite element method software. A uniform temperature distribution at the center of the microheater can be confirmed, and a temperature of  $400^\circ\text{C}$  is attained at the expense of 20 mW of power consumption.

Based on the above-mentioned design, a bulk micromachined microheater is fabricated using a CMOS-compatible MEMS process, as shown in Fig. 1. Multilayers are initially deposited onto a  $500\text{-}\mu\text{m}$ -thick two-sided polished p-type Si wafer, where the resistivity is approximately  $1\ \Omega\text{-cm}$  to  $30\ \Omega\text{-cm}$  and the direction is (001). After forming the multilayers, the deposited Ti/Pt thin film is patterned for the microheater by using a

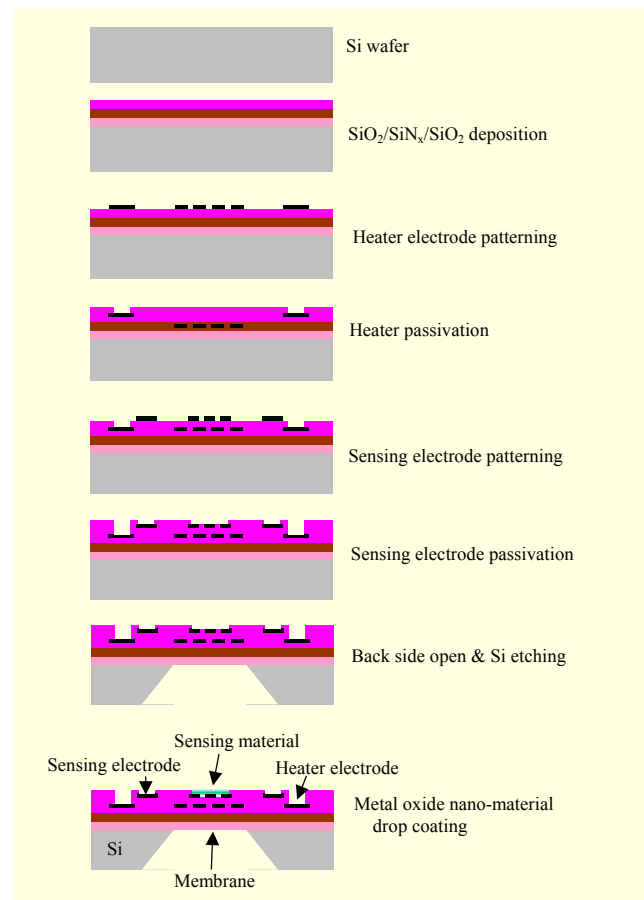


Fig. 1. Fabrication process of micro gas sensor based on CMOS-compatible MEMS process.

lift-off process. To maintain electrical insulation between the heater and gas sensing electrode and to protect the sensing electrode from thermal damage, a  $\text{SiO}_2$  passivation layer is deposited and patterned. We complete the bulk micromachined MEMS microheater using back side anisotropic etching with KOH (40%wt) at  $75^\circ\text{C}$  [18]-[23], in which etching is automatically stopped at the dielectric layer.

Semiconducting  $\text{SnO}_2$  nanopowders are synthesized using a coprecipitation (CPT) method. For a homogeneous CPT process, 0.5 mol/L urea solution is added drop-wise to 0.025 mol/L of  $\text{SnCl}_4 \cdot 5\text{H}_2\text{O}$  solution, which is stirred over a 10-minute period. The mixture is then heated slowly to  $80^\circ\text{C}$  and allowed to react for four hours. The urea decomposes slowly during the release of ammonia and carbonate ions into the solution. The gradual and uniform rise in pH results in nucleation and growth of uniformly sized and shaped particles of the metal oxy-basic carbonate. The mixture is then cooled in an ice bath for three hours. After discarding the supernatant, the precipitate is washed to remove any traces of chloride ions. It is then dried at  $120^\circ\text{C}$ , hand-ground, and calcined in an alumina crucible at  $550^\circ\text{C}$  for two hours to form tin oxide powders.

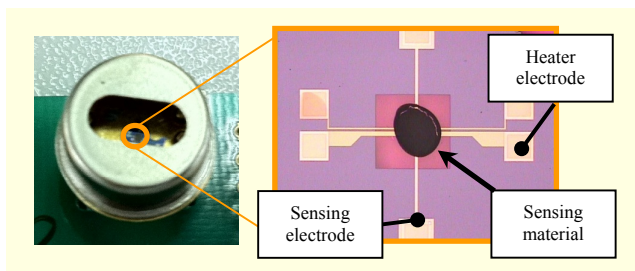


Fig. 2. Photographs of MEMS gas sensor based on SnO<sub>2</sub> nanopowder.

From the calcined SnO<sub>2</sub> nanopowders, to increase the response for CO gas, other metal oxide nanopowders and rare metals are added. Based on the SnO<sub>2</sub> nanopowders, 10%wt WO<sub>3</sub> nanopowders and a 0.5%wt Pt solution are mixed and ball milled with zirconia balls and ethanol for 48 hours. After ball milling, the sensing nanopowders based on SnO<sub>2</sub> nanopowders are obtained by drying for 12 hours at 120°C. The structural properties of the SnO<sub>2</sub> nanopowders are characterized using X-ray diffraction (XRD) and a scanning electron microscope (SEM) analysis.

SnO<sub>2</sub> nanopowders are drop-coated in slurry form, which is a mixture of SnO<sub>2</sub> nanopowders, binder, solutions, and so on. After SnO<sub>2</sub> coating, to obtain a rigid contact between the sensing electrode and nanopowders and to obtain a stable gas detection operation, rapid thermal annealing is performed using an embedded microheater.

A photograph of the metal oxide nanopowder gas sensor is shown in Fig. 2. The photograph is of the packaged gas sensor based on SnO<sub>2</sub> nanopowders. Because the selective metal oxide nanopowder coating process is the final step, the device fabrication process is CMOS compatible.

The current-voltage characteristics are measured using an Agilent 4156C semiconductor precision analyzer. For all metal oxide nanopowder devices, to obtain a rigid contact between the sensing electrode and nanomaterial, rapid thermal annealing is performed using an embedded microheater below 500°C for less than five minutes. The measured current characteristics between the sensing electrodes are sometimes unstable, and the current magnitude is about several pA at 1 V DC bias before annealing. After annealing, the measured current characteristics are always stable and several hundreds of pA at 1 V DC bias at room temperature, as shown in Fig. 3. Therefore, post-annealing nanopowder devices are used for measuring the electrical and gas sensing properties.

The gas sensing properties are measured using a computer-controlled characterization system and PDA based on a Bluetooth technique. The test gases are mixed with air to achieve the desired concentration, and the flow rate is maintained constantly using mass flow controllers. The response is given

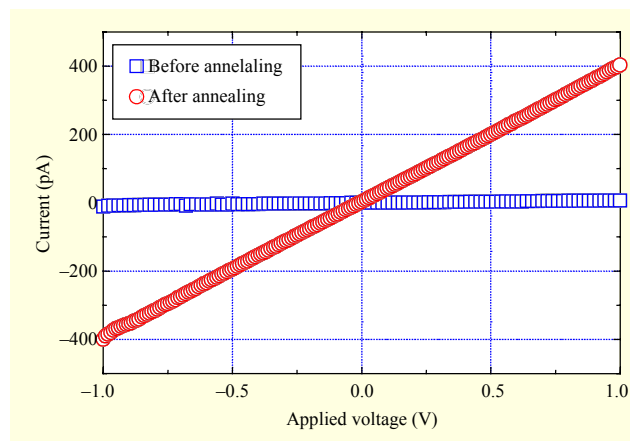


Fig. 3. Measured current-voltage characteristics of gas sensor at room temperature before and after annealing.

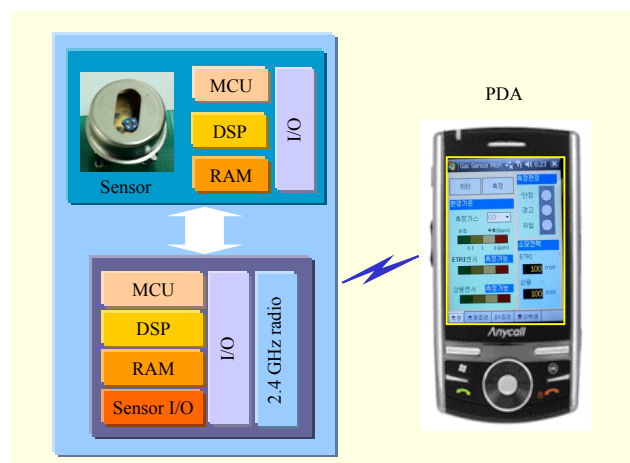


Fig. 4. A schematic diagram of real-time wireless environmental monitoring system including a gas sensor module, Bluetooth module, PDA, and processing program.

by the relative resistance,  $R = \Delta R/R_0 = |R_g - R_0|/R_0$ , where  $R_g$  and  $R_0$  are the resistances in the test gas and air, respectively.

## 2. Wireless System Design and Sensor Integration

A schematic diagram of the real-time environmental monitoring system consists of a sensing unit, communication module, and display module, as shown in Fig. 4. The microprocessor-based sensing unit interfaces with sensors and is capable of acquisition, digitization, and wireless signal transmission using the Bluetooth standard. Due to the necessity for communication of the acquired environmental monitoring results, a PDA phone is adequate for display and communication.

The sensor can be operated using a simple voltage divider in the PDA-based gas sensing measurements. A schematic circuit of the sensor module is shown in Fig. 5.

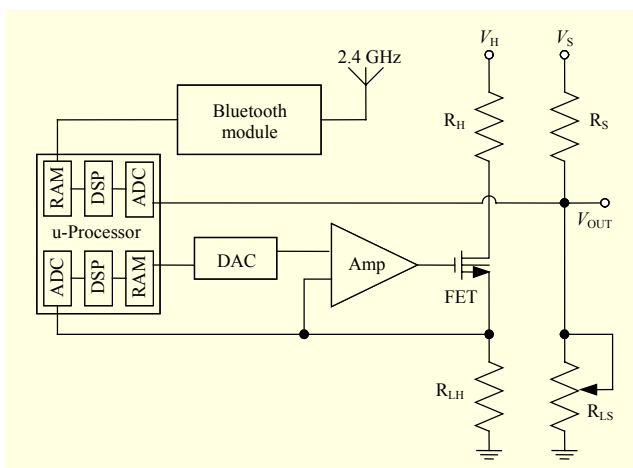


Fig. 5. A schematic circuit for sensor module used to measure gas sensing performance and control operating temperature of developed gas sensor.  $R_H$ ,  $R_S$ ,  $R_{LH}$ , and  $R_{LS}$  are microheater resistance, gas sensor resistance, resistance used to measure current flowing in  $R_H$ , and resistance used to measure  $V_{out}$ , respectively.

This requires two voltage supplies: microheater voltage,  $V_H$ , and circuit voltage,  $V_S$ , where  $V_H$  is applied to the microheater to maintain a constant, elevated temperature for optimum sensing, and  $V_S$  is applied to allow for a measurement of the output voltage,  $V_{out}$ , across load resistor  $R_{LS}$ .

The change in resistance of the metal oxide nanopowder gas sensor is converted into a change in voltage using signal-conditioning circuits connected to the microprocessor unit. The operating temperature of the developed gas sensor is feedback-controlled using a database that shows the given power-dependent microheater temperature, digital/analog converter, field-effect transistor, and microprocessor. The power consumption can be calculated using the data listed above. In addition, the power consumption of the commercial gas sensor embedded in the wireless environmental monitoring module shown in Fig. 6 can be calculated using the voltage and current recommended in a commercial brochure.

To obtain the sensor responses for detecting a gas exposure, sensor-interrogating circuits are made on a small PCB with a size of about  $4\text{ cm} \times 4\text{ cm}$ , photographs of which are given in Fig. 6, in which the front and back sides of the wireless environmental monitoring subsystem using the metal oxide nanopowder gas sensors are shown.

The program interfaces with a serial Bluetooth device at the host controller interface and universal asynchronous receiver/transmitter level. The software is developed on a Microsoft.net platform using Visual C#. It also includes a visual interface to plot the real-time data from different sensor channels on the wireless device. It can also log and save the data in memory for further analysis and comparison.

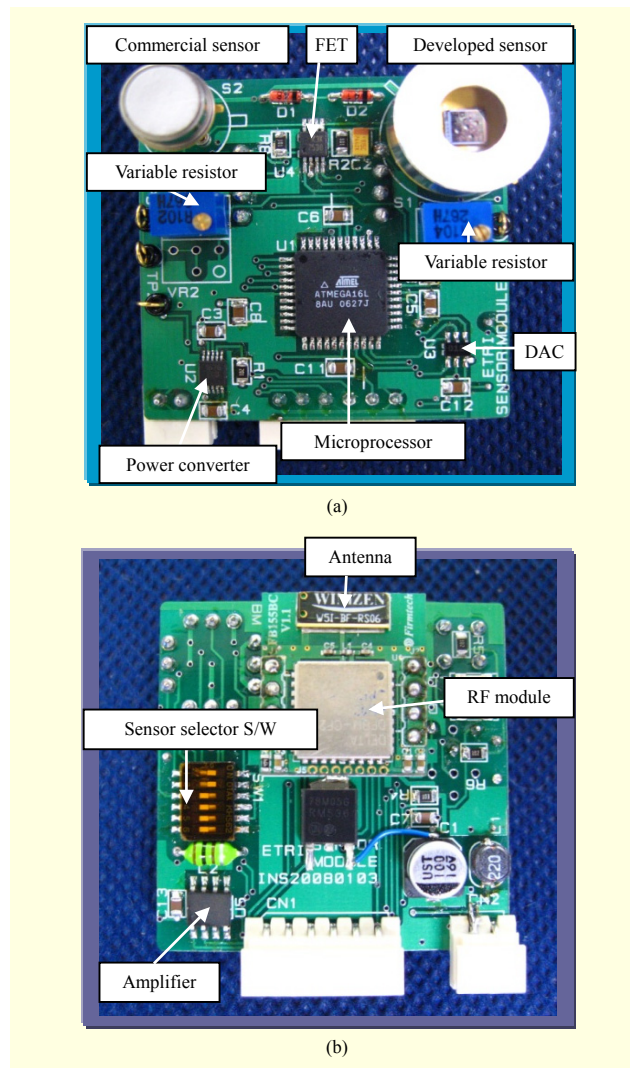


Fig. 6. Photographs of (a) front and (b) back sides of wireless environmental monitoring subsystem using MEMS gas sensor.

### III. Results and Discussion

#### 1. Gas Sensor Evaluation

Various gases, such as  $\text{NO}_2$  and  $\text{CO}$ , have been used in chemical sensing studies. The monitoring of these gases in the environment is of paramount importance. As known, chemisorbed gas molecules on a metal oxide surface withdraw or donate electrons to the conduction channel, giving rise to a conductance change.

The test gas is balanced with dry air, and nitrogen dioxide and carbon monoxide gas concentrations are varied from 0.1 ppm to 5 ppm and from 1 ppm to 50 ppm, respectively, with a fixed carrier gas volume. The above metal oxide material (generally n-type semiconductor) devices exposed to oxidizing and deoxidizing gases show decreasing and

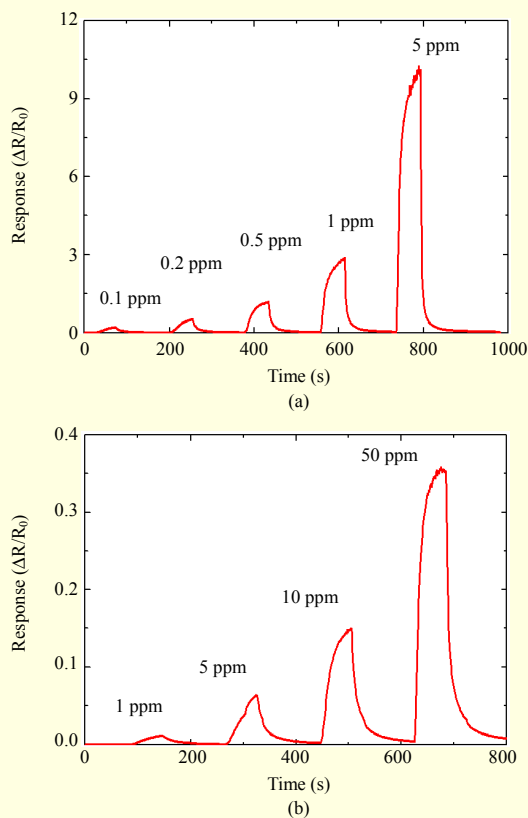


Fig. 7. Gas sensing characteristics of (a) NO<sub>2</sub> gas sensor and (b) CO gas sensor.

increasing conductance, respectively, as the gas concentrations increase. An operating temperature of about 400°C is chosen for the gas sensor. The measured nitrogen dioxide and carbon monoxide gas sensing properties are shown in Figs. 7(a) and 7(b), respectively. An increasing curve with respect to the measured time corresponding to the bottom of the graph represents a change in response. For both cases, the gas sensing response increases under a higher concentration. The sensor device shows responses of about 2.9 and 0.15 for 1-ppm NO<sub>2</sub> and 10-ppm CO, respectively. In addition, the response and recovery times for a 90% response rate are 38 s and 20 s, respectively, for 1-ppm NO<sub>2</sub>, and 39 s and 44 s, respectively, for 10-ppm CO gas. The performance of the above micro gas sensor fulfills the limits for NO<sub>2</sub> and CO pollutants set by the National Ambient Air Quality Standards of the Korean Ministry of Environment, which are 0.1 ppm and 25 ppm [24], respectively.

Despite a variation in base resistance  $R_0$ , several forms of empirical phenomenological formulae describe the dependence of the responses of SnO<sub>2</sub>-based gas sensors on the concentration of various gases [25]. Under a flat band condition, it is known that the formulae assumes the power law form of  $R = K p_g^\alpha$ , where  $R = \Delta R/R_0$ ,  $K$  is a reaction constant,  $p_g$  is the gas

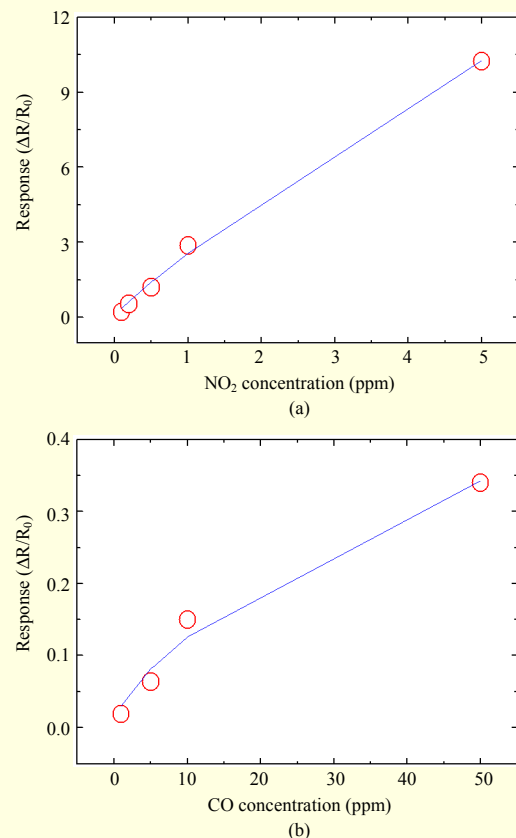


Fig. 8. Gas concentration dependent gas sensing properties for (a) 0.1-ppm to 5-ppm NO<sub>2</sub> gas and (b) 1-ppm to 50-ppm CO gas.

concentration or partial pressure, and  $\alpha$  is an exponent between 0 and 1 [26]. As our sensor, which consists of nanopowders with a thickness of approximately  $\lambda_D$ , may satisfy the flat band condition, it is very likely that the response can be described in the equation above. Figures 8(a) and 8(b) show the dependence of the response on the NO<sub>2</sub> and CO concentrations of the sensor. The data is fitted to the above equation, with  $K = 2.6$  and  $K = 0.03$  and  $\alpha = 0.86$  and  $\alpha = 0.62$ , respectively, where the value of exponent  $\alpha$  differs somewhat according to the nature of the acceptor center [27], [28]. At this high temperature, the gas sensing and desorption are facilitated with an ultra-low power consumption of about 15 mW, which is a benefit of microheater technology. With further optimization efforts, the response and recovery times of our gas sensor can be reduced to much lower levels.

## 2. Evaluation of PDA-Based Environmental Monitoring Subsystem

The operational performance of the PDA-based environmental monitoring subsystem is evaluated through a response test for CO and NO<sub>2</sub> gases. In the environmental

monitoring subsystem, a commercial metal oxide gas sensor is also integrated, and the performances of the gas sensors, including our own, can therefore be tested simultaneously. For example, the microheater power consumption, minimum gas detection limit, gas response time, and so on can be confirmed through the data display on a PDA panel.

To test the operation of the environmental monitoring subsystem, it is placed in a stainless steel chamber through which the test gas based on air gas with the desired concentration will flow. The response detected in the gas sensor is then converted and delivered to the PDA using the Bluetooth module. All measurements of the gas responses are accomplished twice per second successively by saving the response-time profile data, which is composed of the initial stabilized voltages for several seconds, the transformed voltage variation of the given time exposure to each gas, and a recovery profile for the air gas. The measured voltage variations are converted and displayed as gas concentration in the PDA panel through a comparison with the database stored in the PDA, which shows the relation of voltage variations to the detected gas concentration.

The measured multivariate data proceeds with the methods described above, extracting the detection response for each sensor, one made by us and the other by a commercial product. The photograph in Fig. 9 shows the display contents in the PDA when the sensor is exposed to nitrogen dioxide and carbon monoxide. The type of gas, the power consumption, the concentration of the detected gas, and so on are displayed for both our gas sensor and a commercial gas sensor. Figures 9(a) and 9(b) show the sensing response of the developed  $\text{NO}_2$  and  $\text{CO}$  gas sensors for 0.1-ppm  $\text{NO}_2$  gas and 50-ppm  $\text{CO}$  gas, respectively. In both cases, the gas sensing response of our gas sensor is similar to that of the commercial gas sensor, but the power consumption is lower than that of the commercial one.

The subsystem described above can be applied to real-time environmental monitoring around a user having a ubiquitous terminal companion, a ubiquitous sensor network, a smart home, an intelligent automobile, and so on. As an example, a Bluetooth headset with the developed wireless environmental monitoring subsystem having a metal oxide nanopowder gas sensor is shown in Fig. 10. The detected environmental information, such as the nitrogen dioxide or carbon monoxide gas concentration, is displayed on the PDA panel or delivered to the user.

#### IV. Conclusion

Metal oxide nanopowder gas sensors for a compact wireless environmental monitoring subsystem were developed and their experiment results evaluated. The responses of a

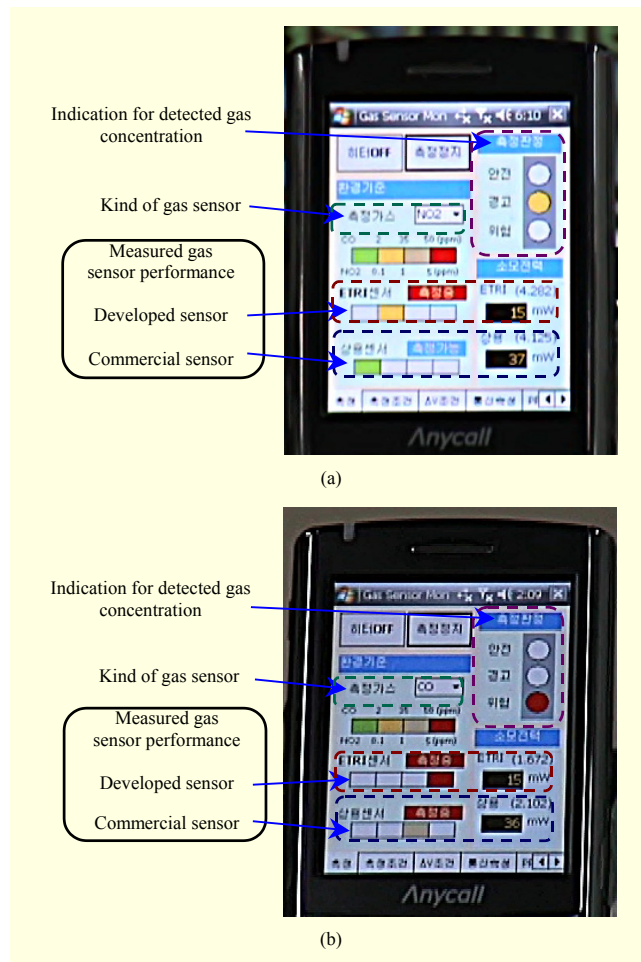


Fig. 9. Photograph of display contents in PDA when sensor is exposed to (a) 0.1-ppm  $\text{NO}_2$  and (b) 50-ppm  $\text{CO}$ , respectively.

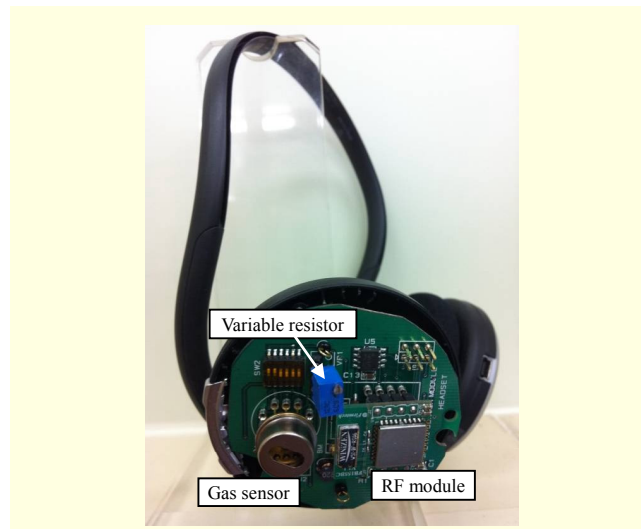


Fig. 10. Photograph of Bluetooth headset with wireless environmental monitoring subsystem having MEMS gas sensor.

semiconductor-type MEMS gas sensor for gases nitrogen dioxide and carbon monoxide were about 2.9 and 0.15 for 1-ppm NO<sub>2</sub> and 10-ppm CO, respectively, with a 15-mW power consumption. The subsystem presented in this paper was developed using a gas sensor module, a Bluetooth module, and a PDA phone. The application of this technology can be extended toward the development of accurate and reliable wireless gas sensors for air quality monitors, automobile exhaust monitors, gas leak detectors, and home food spoilage monitors, among others.

## References

- [1] M. Sharifi and M. Okhovvat "Scate: A Scalable Time and Energy Aware Actor Task Allocation Algorithm in Wireless Sensor and Actor Networks," *ETRI J.*, vol. 34, no. 3, June 2012, pp. 330-340.
- [2] European Environment Agency, "Air Pollution," 2001 Report.
- [3] J. Moon et al., "Semiconducting ZnO Nanofibers as Gas Sensors and Gas Response Improvement by SnO<sub>2</sub> Coating," *ETRI J.*, vol. 31, no. 6, Dec. 2009, pp. 636-641.
- [4] C.S. Moon et al., "Highly Sensitive and Fast Responding CO Sensor Using SnO<sub>2</sub> Nanosheets," *Sensors Actuators B*, vol. 131, no. 2, 2008, pp. 556-564.
- [5] H.G. Byun, K.C. Persaud, and A.M. Pisanelli, "Wound-State Monitoring for Burn Patients Using E-Nose/SPME System," *ETRI J.*, vol. 32, no. 3, June 2010, pp. 440-446.
- [6] J. Jun et al., "A Hydrogen Leakage Detection System Using Self-Powered Wireless Hydrogen Sensor Nodes," *Solid-State Electron.*, vol. 51, no. 7, 2007, pp. 1018-1022.
- [7] A.D. DeHennis and K.D. Wise, "A Wireless Microsystem for the Remote Sensing of Pressure, Temperature, and Relative Humidity," *J. Microelectromech. Syst.*, vol. 14, no. 1, Feb. 2005, pp. 12-22.
- [8] L. Zhao et al., "The Effect of Mutiwallled Carbon Nanotube Doping on the CO Gas Response of SnO<sub>2</sub>-based Nanomaterials," *Nanotechnol.*, vol. 18, no. 44, 2007, pp. 1-5.
- [9] H.K. Lee et al., "Encapsulation of Semiconductor Gas Sensors with Gas Barrier Films for USN Application," *ETRI J.*, vol. 34, no. 5, Oct 2012, pp. 713-718.
- [10] N.J. Choi et al., "Fast Response Formaldehyde Gas Sensor for USN Application," *Sensors Actuator B*, vol. 175, 2012, pp. 132-136.
- [11] S.-J. Kim et al., "Enhanced C<sub>2</sub>H<sub>5</sub>OH Sensing Characteristics of Nano-porous In<sub>2</sub>O<sub>3</sub> Hollow Spheres Prepared by Sucrose-Mediated Hydrothermal Reaction," *Sensors Actuators B*, vol. 155, no. 2, 2011, pp. 512-518.
- [12] D.-S. Lee et al., "Micro Gas Sensor Array with Neural Network for Recognizing Combustible Leakage Gases," *IEEE Sensors J.*, vol. 5, no. 3, 2005, pp. 530-536.
- [13] J. Kong et al., "Nanotube Molecular Wires as Chemical Sensors," *Sci.*, vol. 287, no. 5453, 2000, pp. 622-625.
- [14] D. Zhang et al., "Detection of NO<sub>2</sub> Down to ppb Levels Using Individual and Multiple In<sub>2</sub>O<sub>3</sub> Nanowire Devices," *Nano Lett.*, vol. 4, no. 10, 2004, pp. 1919-1924.
- [15] N. Yamazoe and K. Shimano, "Theory of Power Laws for Semiconductor Gas Sensors," *Sensors Actuators B*, vol. 128, no. 2, 2008, pp. 566-573.
- [16] J.K. Prades et al., "Ultralow Power Consumption Gas Sensors Based on Self-Heated Individual Nanowires," *Appl. Phys. Lett.*, vol. 93, no. 12, 2008, pp. 123110\_1-123110\_3.
- [17] Q. Wan et al., "Fabrication and Ethanol Sensing Characteristics of ZnO Nanowire Gas Sensors," *Appl. Phys. Lett.*, vol. 84, no. 18, 2004, pp. 3654-3656.
- [18] M. Graf et al., "CMOS Microhotplate Sensor System for Operating Temperature up to 500°C," *Sensors Actuator B*, vol. 117, no. 2, 2006, pp. 346-352.
- [19] C. Hagleitner et al., "Smart Single-Chip Gas Sensor Microsystem," *Nature*, vol. 414, 2001, pp. 293-296.
- [20] S.Z. Ali et al., "High Temperature SOI CMOS Tungsten Micro-Heaters," *Proc. IEEE Conf. Sensors*, 2006, pp. 847-850.
- [21] S.E. Moon et al., "Low-Power-Consumption and High-Sensitivity NO<sub>2</sub> Micro Gas Sensor Based on a Co-Planar Micro-Heater Fabricated by Using a CMOS-MEMS Process," *J. Korean Phys. Soc.*, vol. 56, no. 1, 2010, pp. 434-438.
- [22] F. Udrea et al., "Three Technologies for a Smart Miniaturized Gas-Sensor: SOI CMOS, Micromachining and CNTs — Challenges and Performance," *Proc. 2007 IEEE Int. Electron Dev. Mtg. Tech. Dig.*, Washington, DC, Dec. 2007, pp. 831-834.
- [23] S.E. Moon et al., "High-Response and Low-Power-Consumption CO Micro Gas Sensor Based on Nano-powders and a Micro-heater," *J. Korean Phys. Soc.*, vol. 60, no. 2, 2012, pp. 235-239.
- [24] Korean Ministry of Environment, "Air Pollution," 2010 Report.
- [25] N. Barsan, M. Schweizer-Berberich, and W. Gopel, "Fundamental and Practical Aspects in the Design of Nanoscaled SnO<sub>2</sub> Gas Sensors: A Status Report," *J. Annal. Chem.*, vol. 365, 1999, pp. 287-304.
- [26] J. Gardner and P.N. Bartlett, *Electronic Nose: Principles and Applications*, New York: Oxford University Press, 1999.
- [27] N. Barsan and U. Weimar, "Conduction Model of Metal Oxide Gas Sensors," *J. Electroceram.*, vol. 7, 2001, pp. 143-167.
- [28] A. Kolmakov et al., "Detection of CO and O<sub>2</sub> Using Tin Oxide Nanowire Sensors," *Adv. Mater.*, vol. 15, 2003, pp. 997-1000.



**Seung Eon Moon** received his BS, MS, and PhD in physics from Seoul National University, Seoul, Rep. of Korea, in 1990, 1994 and 2000, respectively. Since 2000, he has been with ETRI, Daejeon, Rep. of Korea, working on various application devices based on oxide materials. His current research activities include the development of piezoelectric energy harvesters, MEMS gas sensors, microwave tunable devices, and oxide non-volatile memory.



**Woo Seok Yang** received his BS, MS, and PhD in materials science and engineering from Pohang University of Science and Technology, Pohang (POSTECH), Rep. of Korea, in 1991, 1993, and 1998, respectively. From 1998 to 2001, he worked on FeRAM and DRAM at Hynix Semiconductor Inc. He has been with ETRI since 2001. His recent research interests are in the fields of physical MEMS devices and advanced functional materials.



**Nak-Jin Choi** received his BS from Pukyong National University, Busan, Rep. of Korea, in 1996 and MS and PhD from Kyungpook National University, Daegu, Rep. of Korea, in 1998 and 2005, respectively. Since 2005, he has been working for ETRI, Daejeon, Rep. of Korea, in the area of various application devices based on oxide materials. He has been involved with research on e-nose since 1997 and has conducted research on actuators by polymer.



**Hyung-Kun Lee** is a senior researcher with the Convergence Components and Materials Research Laboratory at ETRI, Daejeon, Rep. of Korea. Prior to joining ETRI, he carried out postdoctoral research with the Center for Smart Supramolecules, Pohang University of Science and Technology (POSTECH), Pohang, Rep. of

Korea, in 2004 and Materials Science and Engineering at Northwestern University, Evanston, IL, USA, from 2005 until 2006. He completed his PhD in chemistry at POSTECH in 2004, studying self-assembly of liquid crystalline materials and supramolecular amphiphiles. His current research interests are mainly focused on gas sensors and nano materials.



**Jaewoo Lee** received his BS in electrical and electronics engineering from Korea University, Seoul, Rep. of Korea, in 2000 and his MS in information and communication engineering from Gwangju Institute of Science and Technology (GIST), Gwangju, Rep. of Korea, in 2002. After that, he joined a micro-systems

team at ETRI, Daejeon, Rep. of Korea, and focused on RF MEMS switches for a front-end antenna module. Since 2006, he has developed MEMS microphones for mobile application.